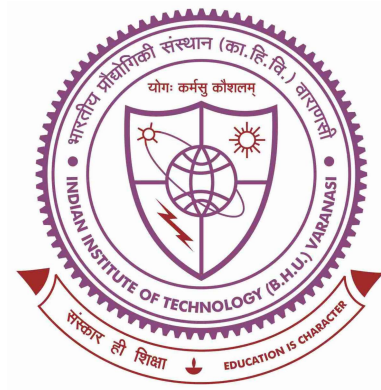


**Development of Scattering Algorithm Through
Polarimetric Decomposition Technique for Surface and
Biophysical Parameters Estimation Using Machine
Learning**



**THESIS SUBMITTED IN PARTIAL FULFILLMENT FOR THE AWARD OF
DEGREE**

DOCTOR OF PHILOSOPHY

in

PHYSICS

by

SHUBHAM KUMAR SINGH

Supervisor

PROF. RAJENDRA PRASAD

DEPARTMENT OF PHYSICS

INDIAN INSTITUTE OF TECHNOLOGY

BANARAS HINDU UNIVERSITY

VARANASI - 221 005

ROLL NUMBER

18171011

YEAR OF SUBMISSION

2023


I would like to dedicate this thesis to my loving parents ...

Certificate

It is certified that the work contained in the thesis titled "**Development of Scattering Algorithm Through Polarimetric Decomposition Technique for Surface and Biophysical Parameters Estimation Using Machine Learning**" by **Mr. Shubham Kumar Singh**, Roll Number **18171011**, has been carried out under my/our supervision, and this work has not been submitted elsewhere for a degree.

It is further certified that the student has fulfilled all the requirements of Comprehensive Examination, Candidacy and SOTA for the award of **Ph.D. Degree in Physics**.

Signature:

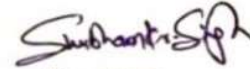

20/11/23
Professor
Department of Physics
Indian Institute of Technology,
(Banaras Hindu University)
Varanasi-221005
Supervisor
Prof. Rajendra Prasad
Department of Physics
Indian Institute of Technology (Banaras Hindu University)
Varanasi-221005 (UP)

Declaration

I, **Shubham Kumar Singh**, certify that the work embodied in this thesis is my own bonafide work and carried out by me under the supervision of **Prof. Rajendra Prasad** from July 2018 to July 2023 at the **Department of Physics**, Indian Institute of Technology (BHU), Varanasi. The matter embodied in this thesis has not been submitted for the award of any other degree/diploma. I declare that I have faithfully acknowledged and given credits to the research workers whenever and wherever their works have been cited in my work in this thesis. I further declare that I have not wilfully copied any others' work, paragraphs, text, data, results, etc., reported in journals, books, magazines, dissertations, theses, etc., or available at websites and have not included them in this thesis and have not cited as my own work.

Date: 20/11/2023

Place: IIT(BHU), Varanasi



Signature:

Shubham Kumar Singh

Certificate by the Supervisor

It is certified that the above statement made by the student is correct to the best of my knowledge.

Signature:

Supervisor

Prof. Rajendra Prasad

Department of Physics

Indian Institute of Technology (Banaras Hindu University)

Varanasi-221005 (UP)

Signature of the Head of the Department

HEAD/विभागाध्यक्ष

भौतिकी विभाग/Deptt. of Physics

संशोधन/कां.हि.वि. /IIT (BHU)

वाराणसी/Varanasi-221005

Copyright Transfer Certificate

Title of the Thesis: "Development of Scattering Algorithm Through Polarimetric Decomposition Technique for Surface and Biophysical Parameters Estimation Using Machine Learning"

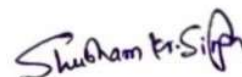
Name of the Student : Shubham Kumar Singh

Copyright Transfer

The undersigned hereby assigns to the Institute of Technology (Banaras Hindu University) Varanasi all rights under copyright that may exist in and for the above thesis submitted for the award of the **Doctor of Philosophy (Ph.D.) in Physics**.

Date: 20/11/2023

Place: IIT(BHU), Varanasi


Signature:

Shubham Kumar Singh

Note: However, the author may reproduce or authorize others to reproduce material extracted verbatim from the thesis or derivative of the thesis for the author's personal use, provided that the source and the Institute's copyright notice are indicated.

Acknowledgements

I would like to express my special gratitude to those people for the constant support, love, and affection I got throughout this journey. Here, I have made a mere attempt to name a few.

First of all, I would like to express my sincere thanks to my respected supervisor, ***Prof. Rajendra Prasad, Department of Physics, IIT(BHU), Varanasi***, for his excellent guidance, continuous encouragement, patience, advice, and moral support during the whole span of my Ph.D. I feel fortunate to have such a supervisor who cared so much about my work, shaped my understanding of the subject, and gave me the confidence to work independently.

I express my cordial thanks to ***Dr. Prashant K. Srivastava, IESD(BHU), Dr. Gulab Singh, IIT(Bombay), and RPEC members Dr. Sunil Kumar Singh, Department of Physics, IIT(BHU), Dr. Shishir Gaur, Department of Civil Engineering, IIT(BHU)*** for their continuous encouragement and support throughout my research work. I express my thanks to all teaching and non-teaching staff members of the Department for their kind support. I wish to thank my fellow lab mates (*Bhagyashree Verma, Sumana Khamrai, Bharat Kumar Prajapati*) of the Remote Sensing Group in the Department for their help and support.

Further, I would like to extend my thanks to my seniors ***Dr. Ajeet K. Vishwakarma, Dr. Ruchi Bala, and Dr. Vijay P. Yadav, Dr. Suraj A. Yadav*** for providing me with a productive environment for carrying out my research work. I would also like to express my sincere appreciation to my colleagues ***Srishti Dixit, Prince Kumar Maurya, Vishal Srivastava*** for their lively friendship and continuous support. I gratefully acknowledge the Department of Science and Technology, Government of India, for providing the ***INSPIRE***

fellowship in the form of a Junior Research Fellowship and Senior Research fellowship through IIT(BHU).

I express my sincere and cordial gratitude to my father *Vijay Kumar Singh*, my mother *Nirmala Devi*, my elder sister *Priyanka Verma*, and my younger brother *Atul Kumar Singh* who always stood by my decisions and provided all kinds of support, moral as well as financial. It was their love, care, and patience that encouraged me to move on.

Department of Physics, IIT (BHU)

Shubham Kumar Singh

Table of contents

List of figures	xx
List of tables	xxv
1 Introduction	1
1.1 Definition of Remote Sensing	1
1.2 Concept and basis of Remote Sensing	2
1.3 Microwave Remote Sensing	5
1.3.1 Wavelength/Frequency	6
1.3.2 Polarization	8
1.3.3 Incidence angle	9
1.4 Optical Remote Sensing	10
1.4.1 Solar Irradiation	11
1.4.2 Spectral Reflectance Signature	11
1.5 Theory and models of electromagnetic backscattering:	14
1.5.1 Biophysical and soil-surface parameters	15
1.5.2 Vegetation Scattering Model	19
1.5.3 Soil-Surface Scattering Model	22
1.6 Literature review	23
1.7 Motivation	28

1.8	Scope and Research Objective	30
1.9	Thesis Outline	31
2	Materials and Methodology	35
2.1	Satellite Data: Key Traits and Attributes	35
2.1.1	Optical data images	35
2.1.2	SAR satellite data	36
2.2	Ground truth data acquisition	40
2.2.1	LAI measurement	40
2.2.2	Soil moisture (m_v) and surface roughness measurement	40
2.3	Methodology	41
2.3.1	Microwave backscattering modelling	42
2.4	Polarimetric Analysis	44
2.4.1	Scattering, Covariance and Coherency Matrix	45
2.4.2	Calculation of different polarimetric index	48
2.4.3	Degree of Polarization	49
2.4.4	Dual Polarized Radar Vegetation Index (DpRVI)	49
2.4.5	Polarimetric radar vegetation index (PRVI)	49
2.4.6	Radar vegetation index (RVI)	50
2.5	Data Fusion	50
3	Synergy of dual – polarimetric radar vegetation descriptor and Gaussian processes regression algorithm for estimation of leaf area index	52
3.1	Introduction	52
3.2	Study area and data used	55
3.2.1	Study area	55
3.2.2	In-situ measurements	56

3.2.3	Satellite data	56
3.3	Methodology	57
3.3.1	LAI estimation based on radiative transfer model within SNAP biophysical processor	57
3.3.2	Computation of dual-polarized radar vegetation index (DpRVI)	58
3.4	Gaussian processes regression (GPR)	59
3.4.1	Performance metrics	60
3.5	Results and discussion	61
3.5.1	Validation of LAI retrieved from SNAP biophysical processor	61
3.5.2	Determination of DpRVI using S1 SAR images	63
3.5.3	LAI estimation using trained GPR-LAI model and validation	63
3.5.4	Sensitivity analysis of the GPR-LAI model	66
3.6	Conclusion	67
4	Incorporation of first-order backscattered power in Water Cloud Model for im- proving the Leaf Area Index and Soil Moisture retrieval using dual-polarized Sentinel-1 SAR data	69
4.1	Introduction	69
4.2	Study area and data used	74
4.2.1	Study area	74
4.2.2	Field data observation	75
4.2.3	Satellite data	77
4.3	Methodology	78
4.3.1	SAR data processing	78
4.3.2	Estimation of vegetation, soil, and interaction scaling constant parameter	79
4.4	Modified WCM model	83

4.4.1	Modified surface scattering Oh model	84
4.5	Vegetation-soil scattering model (VSSM)	85
4.5.1	Parametrization and calibration of WCM	87
4.6	The sensitivity analysis of the proposed mWCM	88
4.7	Results	91
4.7.1	Investigation of relation between vegetation and \mathbf{m}	91
4.7.2	Calculation of backscattering coefficient and WCM inversion	92
4.7.3	Calculation of backscattering coefficients and WCM inversion after including first-order scattering	94
4.8	Conclusion	97
5	An improved volume power approach to estimate LAI from optimized dual- polarized SAR decomposition	102
5.1	Introduction	102
5.2	Study area	105
5.3	Materials	106
5.3.1	Field sampling	106
5.3.2	Satellite	107
5.4	Methods	108
5.4.1	Theoretical background	108
5.4.2	Freeman-Durden decomposition method	110
5.4.3	Odd-bounce and volume scattering	110
5.4.4	Decomposition for dual polarization	113
5.5	Definition of different volume power (VP) indices	117
5.5.1	Volume power modeling	118
5.5.2	Model parametrization and inversion	120
5.6	Results	120

5.6.1	H-alpha decomposition for dual polarization	120
5.6.2	Calculation of degree of polarization	121
5.6.3	Volume power characterization	122
5.6.4	Analysis of VP, DVP, and AVP and retrieval of LAI	124
5.7	Conclusion	126
6	Fusion of optical and SAR data using three approaches for the estimation of LAI with modified Integral Equation model	128
6.1	Introduction	128
6.2	Study area and datasets	130
6.2.1	Study area	130
6.2.2	Satellite data	130
6.2.3	In-situ measurement	131
6.3	Methodology	132
6.3.1	LAI calculation from optical data	132
6.3.2	Simulation of LAI from SAR datasets through WCM	133
6.3.3	Modified integral equation model	134
6.3.4	WCM parametrization and inversion	135
6.3.5	Fusion approach for optical and SAR data	137
6.4	Result and discussion	138
6.4.1	LAI estimation from SAR and Optical data	138
6.4.2	Fusion of LAI estimated from the SAR and optical data	139
6.5	Conclusion	141
7	Conclusion, Summary and Future Work	142
7.1	Conclusion	142
7.2	Summary	143

Table of contents	xix
7.3 Major takeaways from the research	145
7.4 Limitation	146
7.5 Future work	147
References	151

List of figures

1.1	The electromagnetic spectrum.	3
1.2	The impact of the SAR frequency spectrum on the ability to penetrate different surfaces. Greater wavelengths result in increased penetration in different kinds of terrain.	7
1.3	Representations of horizontal and vertical polarizations of a plane electromagnetic wave.	8
1.4	Solar Irradiance Spectra: Above the Atmosphere and at Sea Level	12
1.5	Reflectance Spectrum of Five Land Cover Types.	13
1.6	Standard Vegetation Reflectance Spectrum. Labeled arrows denote key wavelength bands utilized in optical remote sensing of vegetation: A: blue band, B: green band; C: red band; D: near IR band; E: short-wave IR band.	14
1.7	Definition of Leaf Area Index.	16
1.8	Different scattering mechanism over vegetation.	20
1.9	Illustration of Water Cloud Model.	21
1.10	Brief illustration of different soil scattering models.	23
1.11	The phenomenon of reflection and transmission of radar waves when interacting with a planar surface. θ_{i} , θ_{r} and θ_{t} are incident, reflected, and transmitted angles, respectively.	24
1.12	Scattering of electromagnetic radiation from rough surface.	24

2.1	Illustration of measurement of (a) soil moisture through HydraGO device and (b) surface roughness employing plate insertion technique	41
2.2	Different simulation scenarios for different scattering processes.	41
2.3	Interaction between the radar signal and distinct layers.	43
2.4	Components of scattering in model-based decomposition: Surface scattering (Left), Double-bounce scattering (Middle) and Volume scattering(Right).	45
3.1	The location of the district of Varanasi and the study areas in the false-color composite picture created by the S2 image.	55
3.2	Validation of SNAP-derived LAI against ground measured LAI.	62
3.3	Spatio-temporal maps of DpRVI simulated from the dual-polarised S1 SAR datasets for VV-VH polarisation mode.	63
3.4	Validation of GPR-derived LAI from DpRVI and S2 TOA images against in-situ data.	64
3.5	The spatio-temporal maps of LAI from S2 TOA spectral data using trained TOA-GPR. model.	64
3.6	LAI's spatio-temporal maps were obtained from DpRVI datasets using the trained DpRVI-GPR model.	65
3.7	Comparative analysis of estimated LAI using Taylor plot.	66
4.1	Study area showcasing locations (comprising location 1 in red 2 in pink and 3 in yellow) with sampling points, providing a comprehensive view of the entire study region.	75
4.2	The procedure of measuring (a) soil moisture using HydraGO, (b) surface roughness profile.	76
4.3	Temporal variation of ground measured LAI and soil moisture from January to March 2020.	77
4.4	The variation of scaling constant f_{veg} , f_{soil} and f_{inter} shown against the time.	82

4.5	Incorporating the vegetation- soil layer interaction scattering component in the traditional WCM.	85
4.6	Behavior of σ_{veg}^0 (blue), $\tau^2\sigma_{soil}^0$ (green) and $\tau^2\sigma_{inter}^0$ (orange) at VH polarization against LAI with different values of soil moisture (SM), (a) 0.38, (b) 0.25, (c) 0.10 keeping surface roughness (s) and correlation length (l) constant.	89
4.7	Behavior of σ_{veg}^0 (blue), $\tau^2\sigma_{soil}^0$ (green) and $\tau^2\sigma_{inter}^0$ (orange) at VV polarization against LAI with different values of soil moisture (SM), (a) 0.38, (b) 0.25, (c) 0.10 keeping surface roughness (s) and correlation length (l) constant.	90
4.8	The variation of m from January to March 2020. The graphical presentation (upper left) of the m shows that its value decreases as the crop gets denser. The following images are time-series satellite images that illustrate the m 's declining value.	91
4.9	Estimated backscattering coefficient (a) For VV polarization, (b) For VH polarization against SAR backscattering coefficient.	93
4.10	Estimated LAI from model inversion for (a) VV polarization, (b) VH polarization and validated against in-situ datasets.	93
4.11	Estimated SM from model inversion for (a) VV polarization, (b) VH polarization and validated against in-situ datasets.	94
4.12	Estimated backscattering coefficient for (a) VV polarization and (b) VH polarization against SAR backscattering coefficient.	95
4.13	Estimated LAI for (a) VV polarization and (b) VH polarization. Against in-situ LAI.	96
4.14	. Estimated SM from model inversion for (a) VV polarization, (b) VH polarization and validated against in-situ datasets.	96

4.15	The two sets of spatial-temporal maps at (a) VV polarization and (b) VH polarization show the LAI estimation in the large landscape.	98
4.16	The two sets of spatial-temporal maps at (a) VV polarization and (b) VH polarization show the SM estimation in the large landscape.	99
5.1	The image depicts three distinct study sites within the location.	106
5.2	Calculation of scattering power components from modified Freeman-Durden decomposition.	114
5.3	The $H - \alpha$ plane from full-polarization classification. It is divided into distinct zones corresponding to different physical properties.	116
5.4	Temporal variation of the decomposition parameters entropy and alpha of the study region.	121
5.5	Degree of polarization over three study dates for the study pixels over study region.	122
5.6	This figure displays the variations in the volume power behavior of pixels within the designated study region for three different algorithms: (a) FDVP, (b) DVP, and (c) AVP.	123
5.7	Illustrates a comparison between the estimated and simulated volume power within the study region, as obtained through the use of three different imaging techniques: (a) FDVP, (b) DVP and (c) AVP.	124
5.8	The leaf area index (LAI) results were obtained through the use of three different techniques: (a) FDVP, (b) DVP and (c) AVP.	125
6.1	Study area showcasing Location 1 (comprising site 1 in red and site 2 in yellow) and Location 2 with sampling points, providing a comprehensive view of the entire study region.	131
6.2	Evaluation of soil backscattering coefficient's (a) Sensitivity for σ_{soil}^{VH} and (b) Sensitivity for σ_{soil}^{VV} with Gaussian and exponential correlation functions.	135

-
- 6.3 (a) Shows the estimated and observed LAI at VV and VH polarizations
(b) Shows the estimated LAI calculated from PROSAIL RTM and plotted
against the observed LAI. 138
- 6.4 Comparison of LAI estimated from the (a) PCA (b) Regression plotted
against the ground measurements. 139
- 6.5 (a) Shows the accuracy of the estimated LAI from the deep learning against
the ground LAI data. (b) Shows the training and validation loss over time. 140
- 6.6 Spatio-temporal maps showing the variation of LAI at the large landscape. 141